Bearing Faults Classification Using THH and Neural Network

A. KABLA and K. MOKRANI

Department of Electrical Engineering, University of Bejaia, 06000, Bejaia Algeria

Abstract

The induction machine has many advantages: its specific power, its strength, relatively low manufacturing cost and minimal maintenance. But despite all these qualities, a number of faults can affect the life of the machine showing premature failures. The purpose of preventive maintenance in real time, we introduce a new signal processing technique based on Hilbert-Huang Transform (HHT) and marginal spectrum. Firstly, the current signals are decomposed into several intrinsic mode function (IMFs) using the empirical mode decomposition (EMD). The Hilbert Huang spectrum for each IMF is an energy representation in the time-frequency domain using the instantaneous frequency. The marginal spectrum of each IMF can then be obtained. The next step is the classification of faults detected by the application of neural network on IMFs. Tests on real signals show that the marginal spectrum of the second IMFs can be used for the detection and classification of bearing faults. The proposed approach provides a viable signal processing tool for an online machine health status monitoring.

Keywords: *Signal processing, bearing faults, Hilbert-Huang transform, empirical mode decomposition, neural networks.*

1. Introduction

The asynchronous machine occupies an important place in the industry. It is used in many different applications: wind, military, electric drive for high speed train and pumping. To ensure continuity of operation, establishment of maintenance programs are required. Traditionally the maintenance procedure, known as remedy, was to repair or replace faulty equipments. A new approach, called predictive maintenance, is the detection and localization of faults and failures and act earlier to minimize their secondary effects [1]. Studies on the analysis of the current signal (MCSA: Motor Current Signature Analysis) show that in addition to the information contained in the vibrations, information specific to electrical phenomena appears in the stator current signal [2].

Many methods based on the MCSA have been developed. These methods include the assessment of the power spectrum, the fast Fourier transform (FFT), spectrum analysis of the envelope. It turned out that they are effective in the detection of bearing faults. However, they are limited to stationary signals.

To treat non-stationary signals, several time-frequency analysis tools are commonly used such as Fourier transform short-term (STFT) [3], the Wigner-Ville Distribution (WVD) [4], and RTF (Time-frequency representation) of Cohen's class and the wavelet transform (WT) [5]. The main drawback of these methods is that they depend on different parameters. For example, selection of a suitable window size is required when applying the STFT to match with the specific frequency content of the signal, which is generally not known a priori. Wavelets require the specification of a core or a core function. However, there is no universal core. In addition, one limitation of TFR, such as the WVD is the presence of interfering terms which affects the interpretation and readability of the resulting representations [6]. The time-frequency smoothing can reduce interferences but it introduces time and frequency localization errors.

In this paper, we introduce a new approach for analyzing non- stationary signals developed by Huang et al [7]. First the signal is decomposed into several intrinsic mode function (IMFs) using the empirical mode decomposition (EMD). Then the Hilbert transform is applied to each IMF. Therefore, a time-frequency distribution is obtained. The Hilbert-Huang Transform is applied in this paper for detection of bearing faults.

After detection, you go to the classification of these faults is a very important operation for possible intervention in preventive maintenance.

2. Empirical Mode decomposition

The EMD is defined by a sifting process. It can decompose a multi-components signal into a series of IMFs.

Huang et al [7] have defined the IMFs as a function class that satisfies two conditions:

1) At any point, the mean value between the envelope defined by local maxima and the envelope defined by the local minima is zero.
2) The number of extrema and the number of zero-crossings are either equal to each other or differ by at most one.

Copyright (c) 2012 International Journal of Computer Science Issues. All Rights Reserved.

To extract the IMFs, the sifting process used is defined in [7]. Having obtained the IMFs, we apply the Hilbert transform to each IMF.
To calculate the instantaneous characteristics (frequency and amplitude) of each IMF, the analytic signal $z_i(t)$ associated to $c_i(t)$ is used:

$$z_i(t) = c_i(t) + j \cdot H[c_i(t)] \tag{1}$$

where:

$$H\{c_i(t)\} = \frac{1}{\pi} P \int_{-\infty}^{+\infty} \frac{c_i(\tau)}{t-\tau} \cdot d\tau \tag{2}$$

$z_i(t)$ can be expressed by:

$$z_i(t) = a_i(t) \cdot \exp(jw_i(t)) \tag{3}$$

The amplitude and instantaneous phase are defined by:

$$a_i(t) = \sqrt{c_i^{\,2}(t) + H^2[c_i(t)]} \tag{4}$$

$$\theta_i(t) = \arctan\left(\frac{H[c_i(t)]}{c_i(t)}\right) \tag{5}$$

The instantaneous frequency of $z_i(t)$, is simply the derivative of the instantaneous phase:

$$\omega_i = \frac{d\theta_i(t)}{dt} \tag{6}$$

Thus, the original signal can be expressed as :

$$x(t) = Re \sum_{i=1}^{n} a_i(t) exp\left(j \int w_i(t) dt\right) \tag{7}$$

Where the residue r_n was omitted. $\mathrm{Re}\{\cdot\}$ Denotes the real part of a complex quantity.
This time-frequency distribution is designated as the Hilbert-Huang spectrum $H(w,t)$:

$$H(w,t) = Re \sum_{i=1}^{n} a_i(t) exp\left(j \int w_i(t) dt\right) \tag{8}$$

Equation (8) allows us to represent the instantaneous amplitude and frequency in three dimensions, in which the amplitude is the height in the time-frequency plane.
The time integral of Huang-Hilbert spectrum is the marginal Hilbert spectrum $h(w)$ defined as:

$$h(w) = \int_0^T H(w,t) dt \tag{9}$$

where T is the signal duration.

The marginal spectrum offers a measure of the energy at each frequency. It represents the cumulated amplitude over the entire data span in a probabilistic sense.
Therefore, the marginal spectrum of each IMF can be defined, as:

$$h_i(w) = \int_0^T H_i(w,t) dt \tag{10}$$

3. Description

3.1 Principal faults in the machine

A study conducted for IEEE [9], established a statistical flaws that may occur on asynchronous machines; Bearing: 41%, Stator: 37%, Rotor: 10%, and other: 12%.
This distribution shows that faults come mainly from bearings. Faulty bearings causes air gap eccentricities due to irregular motion of the rotor. Theses eccentricities affect the stator current due to the variations of the electromagnetic field.

3.2 Characterization of ball bearings faults

A ball bearing fault is characterized by a continual repetition of faulty contacts with the bearing outer and inner cage. And insofar as the ball bearing supports the rotor, each fault will produce a radial motion of the rotor relative to the stator [10]-[11].

According to *R.Schoen* [12], these variations generate stator currents at frequencies:

$$\left| f_a \pm k.f_{fault} \right| \qquad \text{where : k = 1, 2, 3, …} \tag{11}$$

With: f_a ; power source frequency
f_{fault} ; characteristic frequency induced by the fault.
The characteristic frequencies of the faults depend on the bearing dimensions [2], [12]. The bearing faults can be classified as inner ring, outer ring or ball.

3.3 Description of monitoring system

The tests were carried on the test bed at the LEG Laboratory of Grenoble. The defects were created artificially by an electrical erosion of a 1 mm diameter hole at the outer ring, inner ring or ball [13].

The monitoring system of the stator current used is composed of:
- A three-phase power source with a frequency of 51Hz.

Copyright (c) 2012 International Journal of Computer Science Issues. All Rights Reserved.

- A sampler which aim to acquire the three phase voltages and currents of the stator. After a low pass filtering, signal are sampled at 10 kHz.
- An asynchronous squirrel cage with the following characteristics:

Table 1: Characteristics of the Machine

Parameter	Value
Power	1.1KW
Power Frequency	51 Hz
Motor connection	Y
Phase voltage	400V
Rated speed	1445tr/mn
Number of pole pair	P=2
Number of rotor slots	28
Number of stator slots	48

4. Characterization of bearing fault by HHT

The purpose of this section is to describe the signature bearing fault as it has been observed on the steady state signals. Analyses were performed on blocks of 60000 points; the 10 KHz sampling frequency allows a spectral resolution of $1/6\ Hz$.

4.1 Healthy motor

After having decomposed the healthy signal into IMF the marginal spectrum to IMF 2 and IMF 3 are shown in the following figures:
The marginal spectrum of IMF 2 and IMF 3 are shown in the following figures:

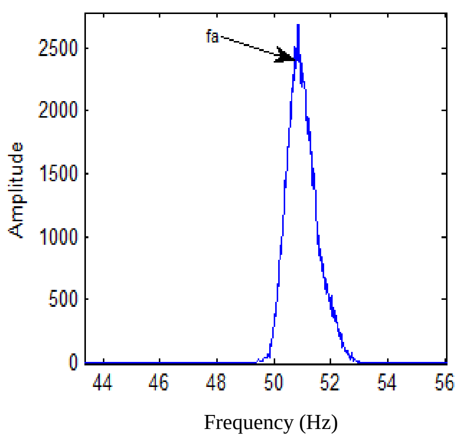

Fig. 1 Marginal spectrum of IMF2

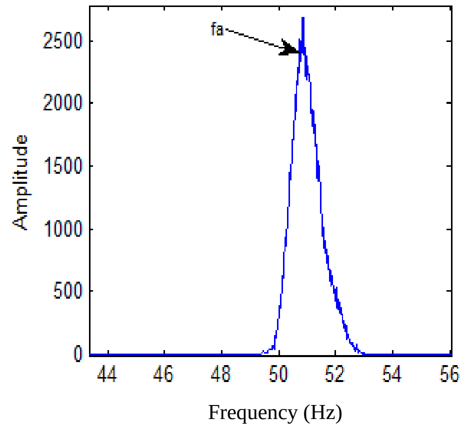

Fig. 2 Marginal spectrum of IMF 3

4.2 Motor with outer race fault

For a rotation speed of 1445 rpm, the theoretical characteristic frequency of this fault is: f_{out} = 76.3 Hz. theoretically it generates, in the stator current spectrum, lines at frequencies shown in table 2.

Table 2: Theoretical frequencies of outer race fault

k	$f_{fault} = \| f_a + k.f_{out} \|$	$f_{fault} = \| f_a - k.f_{out} \|$
1	127.3	25.3
2	203.6	101.6
3	279.9	177.9

The marginal spectrum of the IMF 2 and IMF 3 are shown in the following figures:

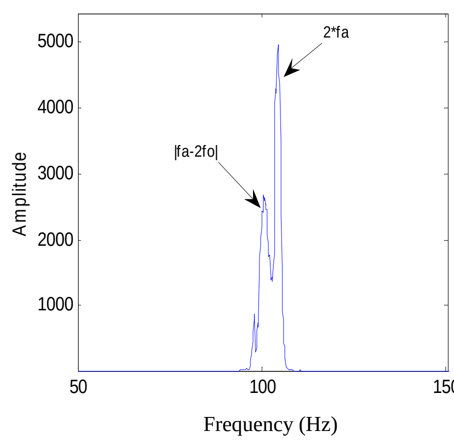

Fig. 3 Marginal spectrum of IMF 2

IJCSI
www.IJCSI.org

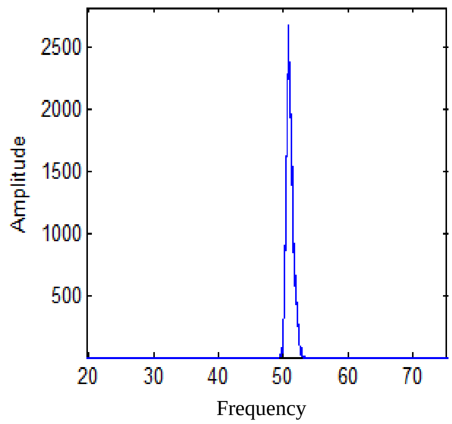

Fig. 4 Marginal spectrum of IMF 3

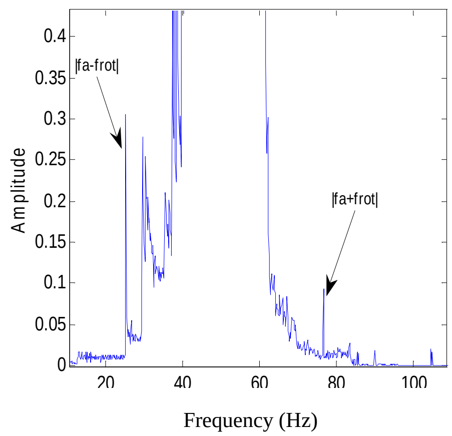

Fig. 5 Marginal spectrum of IMF3 for different frequency range.

4.3 Motor with inner race fault

The cinematic frequency of this fault is f_{in} =124.3Hz. Theoretically, an inner race fault generates spectrum lines at frequencies as shown in table 3.

Table 3: Theoretical frequencies of inner race fault

k	$f_{fault} = \| f_a + k.f_{in} \|$	$f_{fault} = \| f_a - k.f_{in} \|$
1	175.3	73.3
2	299.6	197.6
3	423.9	312.9

The marginal spectrum of the IMF 2 and IMF 3 are shown in the following figures:

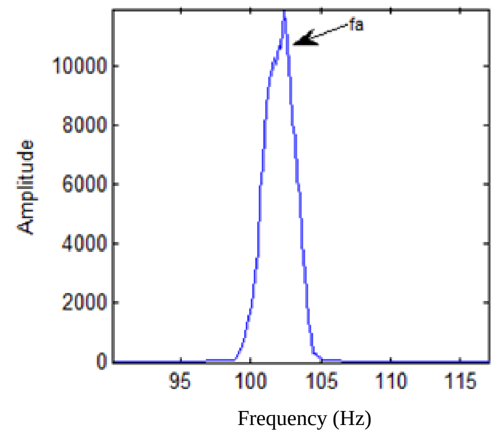

Fig. 6 Marginal spectrum of IMF 2

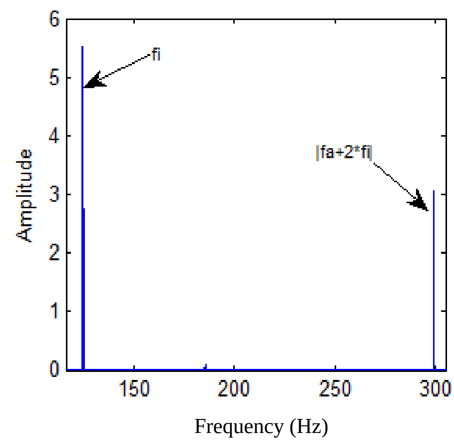

Fig. 7 Marginal spectrum of IMF2 for different frequency range

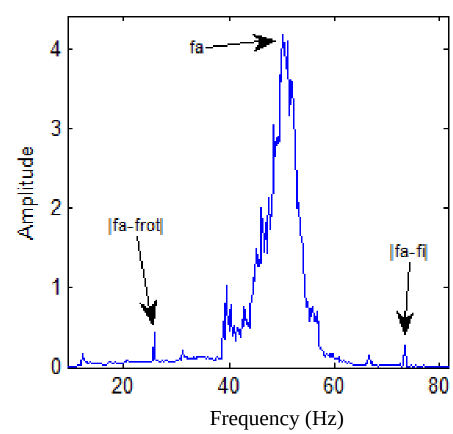

Fig. 8 Marginal spectrum of IMF 3

Copyright (c) 2012 International Journal of Computer Science Issues. All Rights Reserved.

4.4 Motor with ball fault

The cinematic frequency of this fault is f_b = 99.6Hz, theoretically it generates, in the stator current spectrum, lines at frequencies as shown below

Table 4: Theoretical frequencies of ball fault

k	$f_{fault} = \lvert f_a + k.f_b \rvert$	$f_{fault} = \lvert f_a - k.f_b \rvert$
1	150.6	48.6
2	250.2	148.2
3	349.8	247.8

The marginal spectrum of the IMF2 and IMF 3 are shown in the following figures:

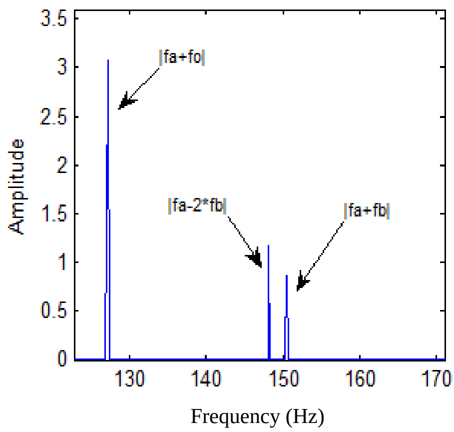

Fig. 9 Marginal spectrum of IMF 2

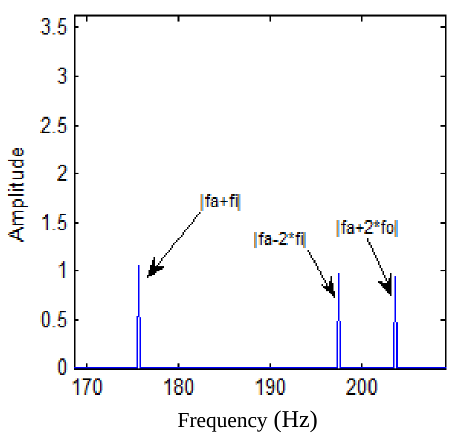

Fig. 10 Marginal spectrum of IMF2 for different frequency range

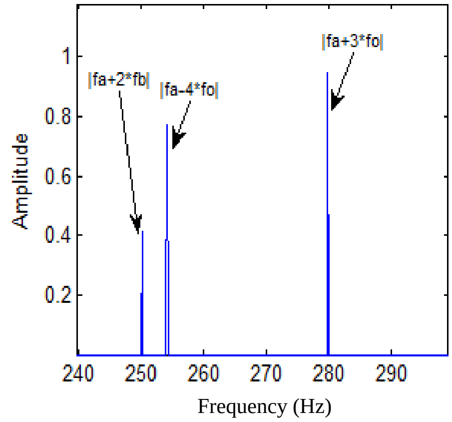

Fig. 11 Marginal spectrum of IMF2
For different frequency range

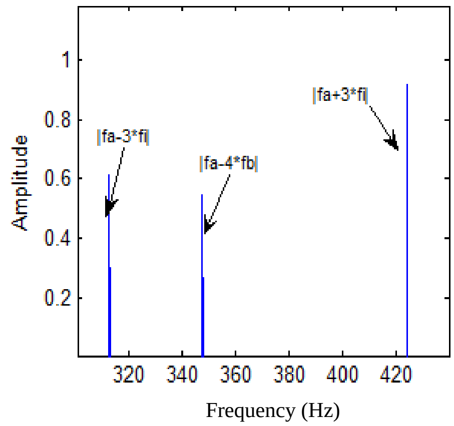

Fig. 12 Marginal spectrum of IMF2
for different frequency range

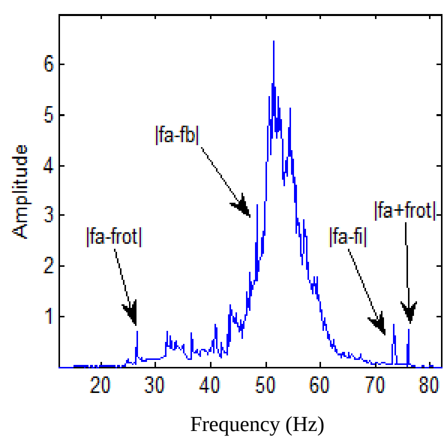

Fig. 13 Marginal spectrum of IMF 3

4.5 Results

From the tests results, we can say that:

Copyright (c) 2012 International Journal of Computer Science Issues. All Rights Reserved.

- bearing faults affect the marginal spectrum of the IMF 2 and 3 of the stator current,
- the ball fault is easier to detect,
- ball faults are characterized by frequencies corresponding to the theoretical outer and inner ring faults. The ball faults can be considered as an outer and inner ring faults [9],
- the amplitude of the ray corresponding to faults is very small compared to the harmonics of the stator current, this could be due to the fact that the faults are not severe enough to generate large amplitude streaks.

5. Implementation of the classification by Neural Network

According to expression (11), a fault creates a frequency shift of the stator current spectrum; this shift is proportional to the characteristic frequency of the fault. We have shown in the previous section that the marginal spectrum of IMF 2 characterizes the bearing fault. We propose to analyze the IMF 2 for the extraction of discriminative features of the faults. The signals of IMFs 2 were represented by their **AR** models; we estimate the order **p** and coefficients **(ai)** of each signal by minimizing the final prediction error (FPE).
To make an automatic classification of the fault we chose the neural network MLP (Multi-layer Perceptron) because it seems suitable for classification problems [14], [15], according to the partition approach. Order p = 4 was set for the parameterization of the test database, so the size of the input of each network is $N_E=4$. The estimated weight for each learns was carried out using standard technique of "back-propagation gradient". To operate this classifier, we adopted a simple decision rule: use of the maximum output found that the class presents.

6. Result of the classification

The classifier contain four sub-networks of hidden neurons and one output neuron each, which are respectively dedicated to the outer race fault class, inner race fault class , ball fault class and healthy class.
After learning from each sub-network (with 400 signals), we performed the test on 80 signals (20 healthy, 20 inner race fault, 20 outer race fault and 20 ball fault). The following figure shows the output of each sub-network according to the test signals.

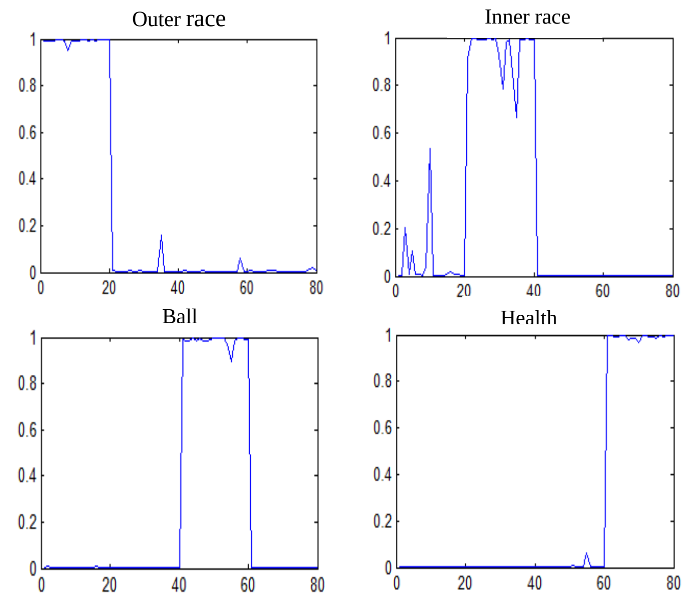

Fig.14 Evaluation of the output of each neural network based on test signals

After applying the decision rule we obtained classification rates as follows:

Table 5: Classification of Fault Rate

	Outer race	Inner race	Ball	Healthy
Outer race	95%	5%	0%	0%
Inner race	0%	100%	0%	0%
Ball	5%	0%	95%	0%
Healthy	0%	0%	0%	100%

- Average classification rate = **98.75%**

6.1. Interpretation

The classification by the partition approach allowed us to obtain very good result. Thus the classification rate obtained is higher than that given in [16] which use the AR model of the envelope of the stator current and neural networks.

7. Conclusion

In this work, to overcome the limitations of traditional time/frequency analysis methods, we applied a new method for the detection of bearing faults in electric machines. The HHT and it marginal spectrum have proven

Copyright (c) 2012 International Journal of Computer Science Issues. All Rights Reserved.

their efficiency for characterizing bearing faults. We can say that the analysis of the stator current using EMD is a promising method which can allows an online monitoring of the electric machine status.

We presented an application of the classification of bearing faults using the AR model to the IMF 2 of stator current and neural networks, which have yielded very interesting classification performance, especially in real time.

References

[1] G. Rostaing, "Diagnostic de Défaut dans les Entraînements Electriques ", Thesis. Grenoble Institute of Technologie, 1997.

[2] F.Tafinine, K.Mokrani, K.Hamasse, "Diagnostic des Machines Asynchrones par l'Analyse Spectrale du Courant Statorique," In Proc. National Conference Electrical Engineering, (University of Tiaret), November 2004, pp. 256-260.

[3] Y. Zhang. " Hilbert-Huang transform and marginal spectrum for detection of bearing localized defects ", IEEE Proceeding of the 6th World Congress on Intelligent Control and Automation, June 21-23, 2006, pp.5457-5461.

[4] W.J.Staszewski, K. Worden, G.R.Tomlinson, "The-frequency analysis in gearbox fault detection using the Wigner-Ville distribution and pattern recognition", Mechanical Systems and Signal Processing, Vol.11, n°.5, pp.673-692, 1997.

[5] H. Sharabaty. " Diagnostic de somnolence d'un opérateur: analyse automatique de signaux physiologiques», Thesis, University of Toulouse, 2007.

[6] J-C. Cexus. "Analyse des signaux non-stationnaire par transformation de Huang, opérateur de Teager-Kaiser, et transformation de Huang-Teager (THT) ", Thesis, Université of Rennes 1, December 2005.

[7] N.E. Huang, Z. Shen, S.R. Long, M.C. Wu, H.H. Shih, Q. Zheng, N.C. Yen, C.C. Tung, H.H. Liu. "The empirical mode decomposition and the Hilbert spectrum for nonlinear end non-stationary time series analysis", Proceeding of the Royal Society of London, 454:903-995, 1998.M. Young, The Technical Writers Handbook. Mill Valley, CA: University Science, 1989.

[8] Q. He, H.J. Zhang, H.L. Zhou. "Evaluation of Stress Using Ultrasonic Technique Based on Hilbert-Huang Transform". International Symposium on Instrumentation Science and Technology, Conference Series 48, pp 106–110, 2006.

[9] IEEE Motor reliability working group, "Report on large motor reliability survey of industrial and commercial installations, " IEEE Trans. on Industry application, vol. IA-21, no. 4, July-August 1985, pp. 853-872.

[10] H.Razik, "Le contenu spectral du courant absorbé par la machine asynchrone en cas de défaillance, un état de l'art ", Review 3 EI, n°29, June 2002, pp. 48-52.

[11] B.Raison, " Détection et localisation de défaillances sur un entraînement électrique ", Thesis, (INPG) Grenoble, September 2000.

[12] R .R.Schoen, T.Habetler, F.Kamran, R.Bartheld, «Motor Bearing Damage Detection Using Stator Current Monitoring,", IEEE Trans. on Industry Applications. vol. 31, no. 6, Nov. 1995.

[13] O.Butscher. " Diagnostic de la Machine Asynchrone ". Electrical engineering, (INPG) Grenoble, September 2001.

[14] B.Li, M.Chow, Y.Tipsuwan, J.Fellow, "Neural-Network-Based motor rolling bearing fault diagnosis, " *IEEE Trans. on Industrial Electronics*, vol.47, no.5, Oct. 2000.

[15] G.Dreffus, J.M.Martinez, M.Samuelides, M.B.Gordon, F.Badran, S.Thiria, L.Herault, *Réseaux de Neurones : Méthodologie et Applications,* Edition Eyrolles, Paris, 2002.

[16] F.Tafinine, K.Mokrani, J.Antoni, "Influence de la charge sur le diagnostic des machines asynchrones" in Second International Conference on Electrical Systems ICES'06, May 08-10 2006, Oum El Bouaghi, Algeria.

Copyright (c) 2012 International Journal of Computer Science Issues. All Rights Reserved.